

## USE OF COMPUTATIONAL FLUID DYNAMICS ANALYSIS OF WIND POWER POTENTIAL OF A MICROSITING

Dalmedson Gaúcho Rocha de Freitas Filho, [dalmedson@mecanica.ufrgs.br](mailto:dalmedson@mecanica.ufrgs.br)<sup>1</sup>

Jefferson Küchle, [jeffkuchle@yahoo.com.br](mailto:jeffkuchle@yahoo.com.br)<sup>1</sup>

Adriane Prisco Petry, [adrianep@mecanica.ufrgs.br](mailto:adrianep@mecanica.ufrgs.br)<sup>1</sup>

<sup>1</sup>Grupo de Estudos Térmicos e Energéticos, Departamento de Engenharia Mecânica, Universidade Federal do Rio Grande do Sul, Rua Sarmiento Leite, nº 425, Porto Alegre – RS, Cep 90050-170

**Abstract:** *This paper presents a study on the use of computational fluid dynamics to simulate the air flow over a complex terrain, in order to investigate the methodology and appropriate models for numerical analysis of wind potential in a microregion. Computational fluid dynamics is not a widely used tool in the wind power industry, mainly because of the high computational requirements, lack of experts and definitions to enable good practices in the use of the tool for micrositing problems. This study shows a methodology to evaluate the local wind potential, through the simulation of wind behavior over complex topography with on-site roughness effects, in a computationally generated domain. The analysis of the atmospheric boundary layer provides great detail on the potential positioning of each wind turbine in a wind farm, which allows for the optimal configuration of the turbines to generate the maximum amount of energy from the available space. The commercial software ANSYS CFX is used in this study. This software employs the finite volume method to solve governing equations. The computational domain is generated from data of SRTM90 (Shuttle Radar Topography Mission) obtained from NASA/NIMA (National Aeronautics and Space Administration and National Imagery and Mapping Agency) and treated with free software TOPOCAL (topographic analysis software). The Computational Fluid Dynamics analysis is developed solving the RANS (Reynolds-averaged Navier-Stokes) equations in steady and transient states and the effects of turbulence in the flow are modeled by the  $k-\epsilon$  model, with maximum residual value of  $1E-5$ . The study is developed on an area around the Tamborete Hill, on the southern coast of Santa Catarina, Brazil, where data from an anemometric station are published. Results are consistent with expected flow patterns, and allow for the velocity distribution to be obtained at any point in time and space of the computational domain.*

**Keywords:** *Wind Potential, Computational Fluid Dynamics, Atmospheric Boundary Layer, Wind Farm, Micrositing.*

### 1. INTRODUCTION

Demand for energy, specifically electricity, has increased dramatically over past 100 years, and the environmental impacts of power generation have led to intensified studies on renewable energy. The widely used practice of burning fossil fuels has had a tremendous negative impact on the environment, and in addition the costs of production are growing as reserves become less accessible. Nuclear power has been adopted in many countries, and this alternative brings great risks, high costs and the unresolved issue of atomic waste. Wind energy is one option with great potential, as it is both clean, renewable and can be distributed locally.

The conversion of wind energy depends on two critical factors; the first is the design of the wind turbine, and second the design of the wind farm. At this stage, it is essential to distribute the turbines to result in the most efficient positioning, which is known as micrositing. To develop this study, it is essential to have a detailed knowledge of wind power potential at each point of the project area. This knowledge, in addition to enabling a more efficient design, also results in greater certainty of the amount of energy which the wind farm is expected to produce, reducing the risk to investors and the regional electrical grid.

The methods used to analyze the wind potential are usually based on data obtained from anemometric stations. Computational models are employed for the projection of velocities expected elsewhere in the region based on the data from the measurement towers. The models most commonly used (such as WAsP – Wind Atlas Analysis and Application Program) do not solve the governing equations completely, but make simplifications that speed up the analysis with a reduced accuracy.

An alternative to improve the accuracy of prediction is the use of numerical modeling based on the solution of the Navier-Stokes equation, Computational Fluid Dynamics (CFD). This methodology is being studied as an alternative by various researchers, such as Stangeoom, 2004. The principal limitations to more effective use of CFD are the high computational requirements, the lack of experts, and unclear methodology for mesh, turbulence modeling and appropriate boundary conditions. To ensure that the system of equations is wholly and accurately solved, a high level of computational power is required.

This paper presents an analysis of the flow of wind over a complex terrain. It includes details of the methodology employed, the definition of the geometry of the terrain and the assumptions adopted for the modeling, mesh settings and turbulence model. The results are discussed and suggestions for continuing work are presented.

## 2. BIBLIOGRAPHIC REVIEW

Wind energy is the kinetic energy of moving air, the wind. Wind energy can vary according to the flow rate or direction of wind. For a better understanding, consider a stream of air with density  $\rho$ , with a velocity  $v$  passing through a surface area  $A$ . The power available in the wind  $P$  can be expressed by Equation 1.

$$P = \frac{1}{2} \rho A v^3 \quad (1)$$

where:

$P$  = wind power;  
 $\rho$  = air density;  
 $A$  = cross section area;  
 $v$  = wind velocity.

The power of wind is proportional to the air density  $\rho$ , the intercepting area  $A$  and velocity  $v$  to the third power.

The troposphere is the atmospheric layer closest to the ground. It is approximately 12 km in height. In this region, the surface of the earth has an important influence on the air flow. It is influenced by shear stress and thermal buoyancy forces due to interaction with the surface of the earth, Coriolis acceleration, the earth's rotation and movement of large scale air mass, such as the geostrophic and thermal winds (GASCH; TWELE, 2002). The boundary layer occurs where air velocity varies as the height changes due to the roughness of the terrain and obstacles on land. A boundary layer model used successfully at lower altitudes is the velocity profile approximated by logarithmic law.

$$v_h = \frac{v^*}{K} \ln \left( \frac{h}{z_0} \right) \quad (2)$$

where:

$v^*$  – friction velocity;  
 $K$  – Von Kármán constant;  
 $h$  – height above ground;  
 $z_0$  – roughness length.

The equation shows that the wind speed increases with the height with a logarithmic distribution.

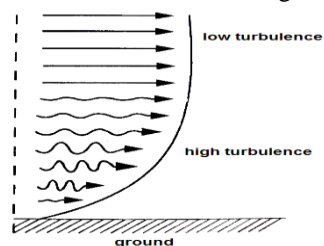


Figure 2.1 Fluid velocity profiles

The wind speed at the any point can be determined analytically by Equation 3 from velocity measurements made at the reference height, and knowing the roughness of the terrain in the region.

$$v_h = v_{ref} \frac{\ln \left( \frac{h}{z_0} \right)}{\ln \left( \frac{h_{ref}}{z_0} \right)} \quad (3)$$

Where:

$h$  – height of interest;  
 $h_{ref}$  – height of measurement obtained;  
 $v_{ref}$  – wind velocity at measurement height;  
 $z_0$  – roughness length.

Table 2.1 shows some values of class and roughness length according to the type of terrain (CUSTÓDIO, 2002).

Table 2.1 – Class and roughness length according to the terrain

Class	Z <sub>0</sub> (m)	Characteristics of the terrain
0,0	0,0002	Seas and lakes
0,5	0,0024	Terrain completely covered with scrub vegetation
1,0	0,03	Terrain with bush
1,5	0,055	Terrain with low density of vegetation and bushes, occurring every 1250m
2,0	0,1	Terrain with vegetation, some distant bushes and small buildings
2,5	0,2	Terrain with small villages, growth of vegetation or bushes
3,0	0,4	Small city, fields with many trees and/or big trees, forest; uneven terrain.
3,5	0,8	Dense suburban area, very uneven terrain.
4,0	1,6	Major city with extremely high-density of tall buildings; extremely mountainous terrain.

### 3. NUMERICAL MODEL

The computational analysis is based on numerical solution of the governing equations of fluid flow. The Finite Volume Method (MALISKA, 1995) is adopted to solve Reynolds Average Navier-Stokes (RANS) equations. RANS equations are obtained by considering the average of time intervals large enough for the study of turbulence; models of turbulence are introduced to represent the total effects in a turbulent flow (WILCOX, 2004). The convergence criteria adopted is 1E-5. The turbulence model used in the simulations is the  $k-\varepsilon$ , defining  $k$  as the kinetic energy of the fluid, and  $\varepsilon$  the dissipation of kinetic energy. The  $k-\varepsilon$  model works with the gradient diffusion hypothesis to relate the Reynolds stresses to average speed and turbulent viscosity. The turbulent viscosity is defined as the product of turbulent velocity and turbulent length scale.

### 4. LOCATION

The microregion chosen belongs to the state of Santa Catarina, southern Brazil, and is situated within the municipality of Laguna on the coast of Santa Catarina. According Dalmaz (2007), the local climate has good wind potential. In the Figure 4.1 is shown the study region.

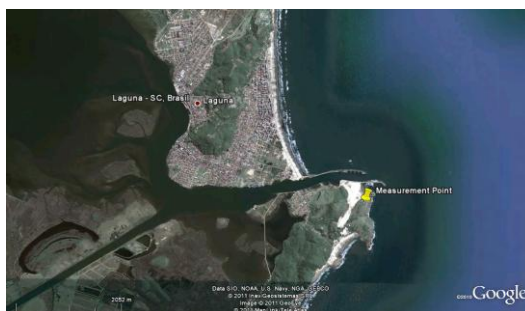


Figure 4.1 Satellite image of the region of Laguna – SC (Source: <http://maps.google.com.br>)

#### 4.1. Wind Data

According to the Brazilian Wind Atlas, it is observed that the coastal region of southern Brazil has a high wind potential. The work presented by Dalmaz (2007) shows great wind potential in this region. These studies present values from two data sources. They are predictions of wind on the mesoscale model, called ETA, from the Center for Weather Forecasting and Climate Studies (CPTEC/INPE) and wind measurement data by CELESC (“Centrais Elétricas de Santa Catarina”).

The data for estimating the wind in mesoscale from CPTEC/INPE has a resolution of 40 km x 40 km. This is considered a low resolution for analysis of a microregion. Data provided by CELESC were obtained by anemometric towers at a height of 30 and 48 m above ground in various localities of the State of Santa Catarina. An anemometer tower is located on Tamborete Hill in the city of Laguna, at coordinate: 28° 30' 2.7" S; 48° 44' 55.5" W. The station is instrumented with a measuring system consisting of two anemometers, manufactured by NRG 40. The acquisition system is a data logger tag NRG-9200 plus. Its measuring range is between 0 to 97,3 m/s. The measurement uncertainty is 0,4 m/s and resolution of 0,1 m/s. Credited with uncertainty in angle of 1,4°. This equipment enables the data storage of average speed, average direction angle and respective standard deviations. The sampling time can be chosen between 10 to

60 min. For all measurements an interval of 10 min was used. These averages are calculated from data processed every 2 sec. The verification of the calibration of anemometers, indicated by the manufacturer, was made in LAC– Aerodynamics Laboratory Construction, in the Federal University of Rio Grande do Sul, according to Silva et al (2004). The data obtained with averages of 10 min are ideal for studying the wind potential of the site. With average speed at intervals between 10 min to 2 h can be a good distinction between large-scale variations and micro-scale, due to turbulence or gusts, Molly (2005). Wind data from the town of Laguna was collected on both a monthly and annually basis. The following figure shows the annual average speeds (DALMAZ, 2007).

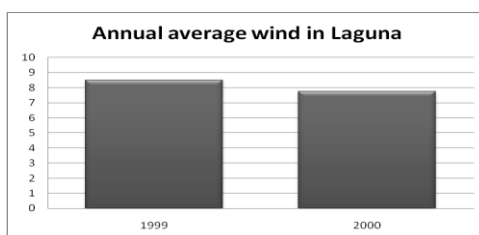


Figure 4.2 Annual average wind in Laguna (Source: DALMAZ, 2007)

The predominant wind direction is very important for the implementation of the wind simulation. The smaller the variation of the wind direction, best results can be obtained, because it is required for each measurement of wind direction. Below, Figure 4.3 shows the direction of incidence of the predominant wind at the measuring station for two consecutive years.

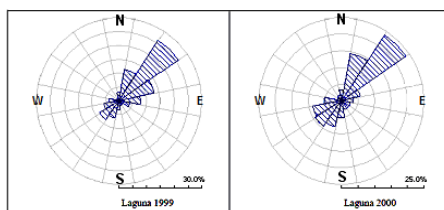


Figure 4.3 – Incidence Wind direction in Laguna (source: DALMAZ 2007)

In Figure 4.3 it can be observed that the main wind direction in Laguna is from the north-east.

## 5. COMPUTATIONAL DOMAIN

The computational domain is defined as a volume with a rectangular base and constant height around the anemometric station of the Tamborete Hill. One side is oriented to the north-east, perpendicular to the predominant direction of the wind in the region. Thus the wind, or flow, enters from the north-eastern end of the domain adopted. The topography of the ground is modeled over the rectangular base.



Figure 5.1 – Location Modeling

The digital terrain model (MDT) is employed. MDT is generated using data from SRTM 90 (Shuttle Radar Topography Mission) by NASA/NIMA (National Aeronautics and Space Administration and National Imagery and Mapping Agency) in 1999, processed and distributed by publicly by National Map Seamless Data Distribution NMSDD of USGS (United States Geological Survey). It consists of an array of elevated terrain points obtained from triangulation of radar in the shuttle coupled.

The original data were obtained on dot matrix with 3 arc sin resolution, about 90m horizontally, and resolution of 1 ft, 33 cm, vertically. This mesh was changed to a horizontal resolution of 50m, for better

softening of the terrain without loss the resolution in dot matrix. The final coordinate system is UTM (cartographic system plan), the time zone -22J, with SAD-69 datum. These points are triangulated in order to form a surface with the free software *Topocal* ([www.topocal.com.br](http://www.topocal.com.br)). The triangles have side dimensions of approximately 50m and are adjusted using the program with the best fit to the points. The next treatment is performed with *SolidWorks 2010*. From the triangle mesh, curved surfaces are created which soften the contours and form the solid terrain of the simulation. The discretization in finite volumes is performed using *Ansys ICEM*. The mesh is an unstructured mesh with prismatic layers near the ground, that best approximate the ground contours. Tetrahedrons differently spaced are obtained, always aiming to have smooth aspect ratios. The prisms on the base are in the highest speed variation of the boundary layer, and tetrahedrons are located in regions of less variation.

### 5.1. Domain and Boundary Conditions

The simulation domain has dimensions of 6500 x 7500m. It has an overall height of eight times the tallest obstacle. The lateral boundaries are at least 500m away from any mountain. The outlet face is 2000m away from the nearest obstacle in this region and the face of inlet remains unchanged. The micro-region of interest is in the center area of the domain so that it is not influenced by boundary conditions.

The boundaries of lateral limits and upper limit of the domain are defined as shear-free wall. It is a reasonable consideration, because the flow is parallel to the plane of the boundary. An outlet condition of zero static pressure is adopted. Thus, the fluid can leave the domain without restriction to the flow. A logarithmic velocity profile with a speed of 7 m/s at a height of 50m above sea level is adopted as the inlet condition. The flow enters the domain from the north-east face (NE) in the open sea region, with an imposed turbulence intensity of 5%. Over the surface of the ground, the no-slip condition of wall is imposed, with different roughness height for two distinct terrains. At sea, according to Table 2.1, a roughness height of 0,0002m is adopted. A roughness height of 0,4m is applied to the hill and city regions, consistent with low buildings and high vegetation from Table 2.1.

## 6. RESULTS

Simulations of the air flow over the micro-region are obtained solving RANS equations with  $k-\varepsilon$  model with convergence criteria adopted is  $1E-5$ . Velocities at any point over the domain are obtained. The results are presented in this section as velocity planes at different height above the sea level or as velocity profiles at different points of study. One important point analyzed is the point corresponding of the position of the anemometric station of Dalmaz (2007) where the influence of the hill in the wind speed measured can be analyzed. The first point to be presented in this chapter is a discussion about mesh quality.

### 6.1 Mesh Quality

Four different meshes of the same structure, with more or less refined elements, are used to verify mesh quality. Simulations are performed with software *Ansys CFX V.12*, with the same boundary conditions in order to verify the behavior of the meshes.

Table 6.1 lists the number of mesh elements with the wind speed on the Tamborete hill at 88m above the sea level, the height at which the anemometer is located (Dalmaz,2007), and also the computed average wind speed at the outlet of the domain.

Table 6.1 Mesh quality with varying number of elements

Mesh Size Number of Elements	Velocity at 40m Tamborete Hill	Average Speed Outlet
249.497	7,812 m/s	8,12488 m/s
421.941	7,716 m/s	8,12430 m/s
927.826	7,705 m/s	8,12493 m/s
1.542.677	7,778 m/s	8,12534 m/s

Data in the table above are shown in Figure 6.1

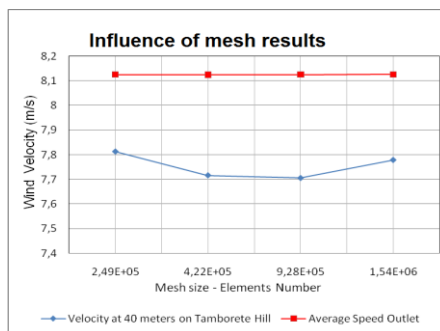


Figure 6.1 Influence of mesh results

From the data presented in Table 6.1, it can be verified that the influence of the mesh in the average velocity at the outlet plane is negligible. The velocity at the point of the anemometer vary below 1% for the two most refined meshes, although the small differences of values the 1.542.677 volumes mesh is adopted.

## 6.2. Velocity Horizontal Planes

The behavior of the wind and perturbation due to the topography at different heights may be observed in horizontal velocity planes shown in this section. Slices at 50, 100 and 150m above sea level are shown, and the influence of the topography is observed. Figure 6.2 presents the topography of the terrain simulated for the computational analysis, over the plane at the sea level.

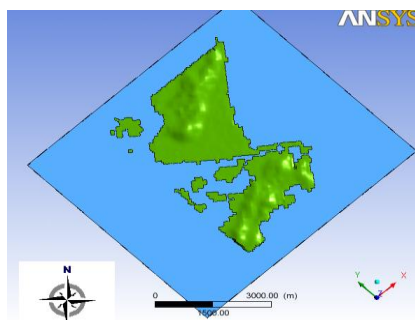


Figure 6.2 Domain simulation

### 6.2.1. Slice at a height of 50m

The slice positioned at a height of 50m above the sea level is, as expected, the most influenced by topography, as shown in the velocity intensity distribution over the plane presented in Figure 6.3. In Figure 6.3, it is possible to verify that the hills exceed a height of 50m.

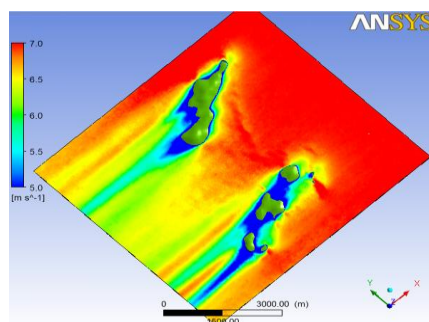


Figure 6.3 Velocity slice at 50m above sea level

Figure 6.3 shows that the aerodynamic wake from the hills extends for 4 km and leaves the area. The wake regions are characterized by high turbulence levels and velocity deficits. The installation of a wind turbines in these regions are not recommended because there may be fatigue of structural and mechanical components due to turbulence, besides the loss of available power. The velocity obtained from the simulation is about 5,5 m/s and flow over the sea at the inlet is 7m/s for the same height. The reduction in wind speed is about 22%, and there is a reduction of 52% in terms of available wind power.

### 6.2.2. Slice at a height of 100m

Figure 6.4 presents velocity intensity distribution at a height of 100 m above sea level. It can be observed that few points in the region exceed the height of 100m. The hill located at the center of Laguna has an approximate height of 125m.

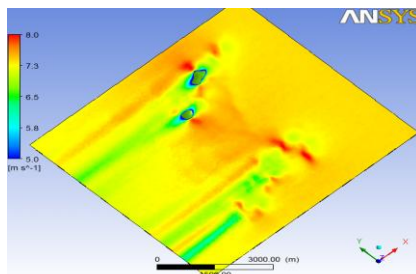


Figure 6.4 Velocity slice at 100m above sea level

At this height, the wakes from the hills are not as intense as seen in the 50m slice. The development of the wakes result in regions with velocities around 6,5 m/s, while non-perturbed flow has 7,39 m/s. The wakes extend for a considerable distance. In the simulation the disturbed area has 4 km further to the hills of the micro-region. The reduction in wind speed is about 12%, and there is a reduction of 32% in terms of available wind power. The regions close to the hills are not suitable for wind turbine installations at the 100m height level.

### 6.2.3. Slice at a height of 150m

The velocity intensity plane at a height of 150m is presented in Figure 6.5. This plane is located above all hills located at the area. The most important feature observed in the figure, is the acceleration of wind at the points over the hills and small reduction of velocity after the obstacles. Hills with smooth curves accelerate the flow over itself.

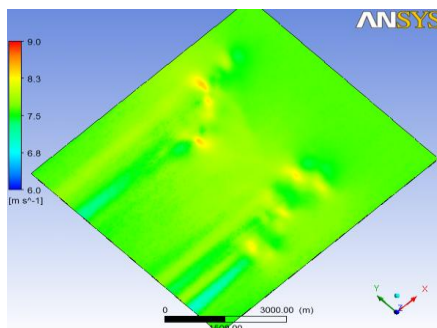


Figure 6.5 Velocity slice at 150m above sea level

### 6.3. Boundary Layer Profiles

In few points, the velocity profile is given to enable to verify the change of wind speed with height, elevation z. In Figure 6.6, the velocity intensity for a vertical slice is presented and the boundary layer can be observed.

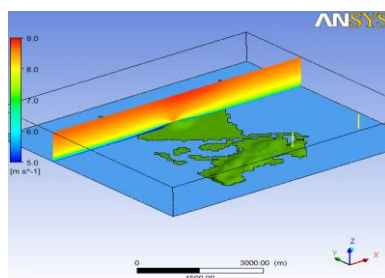


Figure 6.6 - Velocity intensity at a vertical slice.

The slice in Figure 6.6 is positioned in line with the flow passing over the tallest hill in the region.

### 6.3.1. Velocity Profile on the Tamborete hill

The velocity profile in the Tamborete hill is that which relates the measurements presented by Dalmaz (2007), with data obtained by simulation. Dalmaz (2007) presents data of anemometers installed at 48 and 30m over the Hill. At a point 40 meter high above sea level. Figure 6.7 presents the velocity profiles at the location of the measurement station, from 40 to 540m above the sea level, or 0 to 500m from the surface of the hill, as well as the unperturbed velocity profile, obtained at the open sea 2 km before the hill, between 0 and 500m above the sea level. Both profiles of Figure 6.7 are taken from the same slice, which runs parallel to the direction of the wind.

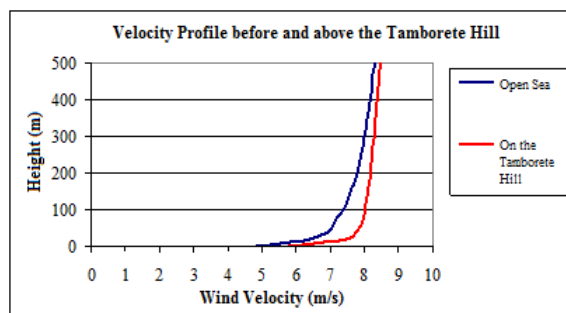


Figure 6.7 Velocity profiles at Tamborete Hill and unperturbed profile above open sea. Height is measured from the ground surface at each point.

The results shown in Figure 6.7 indicate that there is a significant acceleration in wind speed at the location of the measurement station located on the hill. The velocity determined at 48m above sea level of the open sea profile is observed to be 6.9 m/s, while at the same height above the ground surface at the location of anemometer the speed obtained in the simulation is 7.8 m/s, which results in an increase of 11.56%. Moreover, when comparing the velocity profile in the sea to 88m high, it can be observed that the speed of 7.32 m to 7.8 m/s obtained at 88m above sea level at the measuring point, an increase of 6.58%. In Figure 6.7, it can be observed that the inclination of the velocity profile is changed in the region over the hill, and the projection of the values obtained at a height of 48m should not be made from the logarithmic law with the same values of roughness length on plain grounds.

### 6.3.2. Velocity Profile on the tallest hill of the micro-region

Velocity profiles at three locations along the same slice, which passes over the tallest hill in the region, are presented in Figure 6.8. These include a location at the open sea, 3 km before the hill, a location on the hill and another location 3 km after the hill. The profiles are plotted from 0 to 500m height measured above the ground for each location.

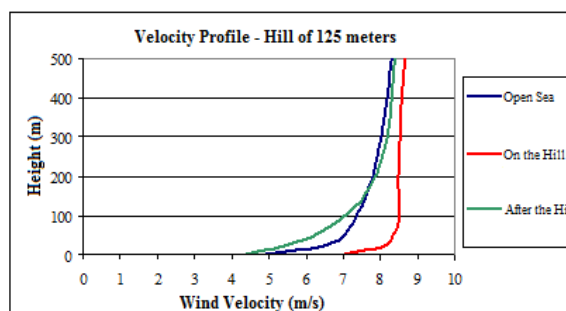


Figure 6.8 Velocity profile before hill, on the hill and after the hill

In Figure 6.8, it is possible to observe the acceleration of the flow on the hill. At the higher altitudes there is an approximation of velocities. The velocity profile after the hill has a lower speed at altitudes below 150m. After 150m it has a small acceleration when compared to unperturbed profile, around 0.25 m/s.

### 6.3.3. Velocity Profile in Laguna town

Profiles plotted in Figure 6.9 show the effect of roughness of the city on the flow. The three velocity profiles are along the slice that cuts through the urban region, from an altitude of 0 to 500m above the sea



level. The Laguna town is located between two hills in the micro-region study. The prevailing wind direction is northeast (NE).

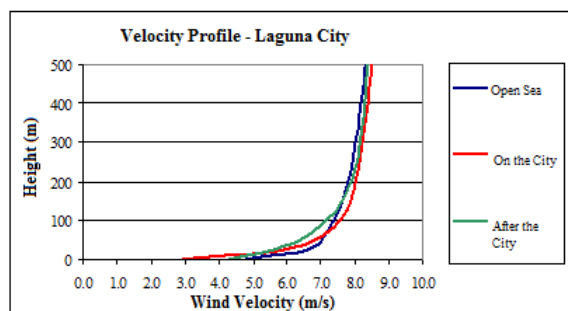


Figure 6.9 Three profiles of wind speed passing over the city of Laguna

In Figure 6.9 it is possible to observe that there is deceleration in the flow at heights less than 60m, and an acceleration at heights over 60m. There is no evident acceleration of the velocity in this flow line, thus the effect of necking of the flow due to the hills does not be observed.

## 5. CONCLUSIONS

This work presents numerical simulation of wind over a complex terrain. The finite volume method with the commercial code ANSYS CFX is used to solve Reynolds Averaged Navier-Stokes equations, with  $k-\epsilon$  turbulence model. TOPOCAL free software is employed to describe the geometry corresponding to the ground topography based on data from SRTM 90 - NASA/NIMA. The rectangular based volume that defines the domain is discretized in a 1.542.677 tetrahedral and prismatic finite volumes mesh. The study is developed on an area around the Tamborete Hill, on the southern coast of Santa Catarina, Brazil, where data from an anemometric station are published (DALMAZ, 2007).

Total height of the domain is defined as eight times the height of tallest hill in the micro-region. As presented in the study of Xiao et al (2010) the boundary of domain must be far from the region of analysis, then the lateral limits are at least 500m far the area in focus.

Results are coherent with the expected behavior of the flow. The aerodynamic wake of hills are obtained as the acceleration on top of obstacles. At a height of 50m above sea level, occurs the greatest reduction in wind speed and power available, especially in regions within the domain of 4 km<sup>2</sup> located downstream the hills. At a height of 100m, there is a small reduction in wind velocity and power. In the plane positioned at 150m wakes are almost inexistent although acceleration on top of high hills is evident.

The velocity Profile along height coordinate on specific points presents the boundary layer development and its modification due to the topographic and roughness local conditions. The results indicate that the velocity distribution over the top of the hill in which the measurement station is positioned is accelerated near the ground. The obtained profile demonstrates that inclination of the curve is also modified and the logarithmic profile with same parameters as used for plain ground is not adequate to provide boundary layer distribution. Results are analyzed only in qualitative way.

The results of the present simulation demonstrate that coherent results may be obtained with the methodology presented in this study adopted; however more research work is required to verify the results quantitatively. The domain dimensions must be studied to verify the influence of boundary in results. The best turbulence model also must be investigated. Validations with experimental results are fundamental to define best practices and research on experimental/numerical analyses which are currently being developed.

## 7. ACKNOWLEDGEMENTS

Authors would like to thank the National Center for Supercomputing - Southern Region, Federal University of Rio Grande do Sul (CESUP-RS/UFRGS).

Dalmedson G. R. de Freitas Filho is also grateful to CAPES- Ministry of Education, Brazil, for granting his a fellowship.

## 8. REFERENCES

- Amarante, O. A. C; Brower, M.; Zack, J.; Sá, A. L. de. Atlas do potencial eólico brasileiro. Brasília, 2001.
- Burton, T.; Sharpe, D.; Jenkins, N.; Bossanyi, E.; Wind Energy Handbook, - John Wiley & Sons, 2001.
- Carcangiu, C. E., 2008. "CFD-RANS Study of Horizontal Axis Wind Turbines", PhD Thesis, Università degli Studi di Cagliari, Itália;
- Carvalho, P., Geração Eólica. Fortaleza: Imprensa Universitária, 2003.

- Castro, Rui M.G. Introdução à Energia Eólica. Universidade Técnica de Lisboa, 2008. 88p.
- Custódio, R. S., Parâmetros de Projeto de Fazendas Eólicas e Aplicação Específica no Rio Grande do Sul. Dissertação (Mestrado em Engenharia Elétrica) – Pontifícia Universidade Católica do Rio Grande do Sul, Porto Alegre, 2002.
- Dalmaz, A., Estudo do Potencial Eólico e Previsão dos Ventos para Geração de Eletricidade em Santa Catarina. Tese de Mestrado, Curso de Pós-Graduação em Engenharia Mecânica, Universidade Federal de Santa Catarina, Brasil, 2007.
- Gasch, R.; Twele, J., 2002, “Wind Power Plants: Fundamentals, Design, Construction and Operation.” Berlin: Solarpraxis AG.
- Küchle, J. Emprego da Dinâmica dos Fluidos Computacional na Análise do Potencial Eólico de uma Microrregião em Laguna. 2010. 20f. Monografia (Trabalho de Conclusão do Curso de Engenharia Mecânica) – Departamento de Engenharia Mecânica, Universidade Federal do Rio Grande do Sul, Porto Alegre, 2010.
- Maliska, C. R. Transferência de Calor e Mecânica dos Fluidos Computacional. LTC, Rio do Janeiro, Brasil, 1995.
- Molly, J. P. Centrais eólicas: técnicas, planejamento, financiamento, verificação. In: CURSO DE ENERGIA EÓLICA, 2005, Fortaleza – CE, maio 2005.
- Petry, A.P., 2002. “Análise Numérica de escoamentos Turbulentos Tridimensionais empregando o Método dos Elementos Finitos e Simulação de Grandes Escalas”, Tese de Doutorado, Curso de Pós-Graduação em Engenharia Mecânica, Universidade Federal do Rio Grande do Sul, Brasil, 2002.
- Piccoli, G. L. Análise da Viabilidade de uma Fazenda Eólica Empregando Dinâmica dos Fluidos Computacional. Monografia (Trabalho de Conclusão do Curso de Engenharia Mecânica) – Departamento de Engenharia Mecânica, Universidade Federal do Rio Grande do Sul, Porto Alegre, 2006.
- Silva, G. K. da; Passos, J. C.; Colle, S; Reguse, W; Beyer, H. G. Metodologia de avaliação do potencial de geração eólica para o estado de Santa Catarina. In: III CONGRESSO NACIONAL DE ENGENHARIA MECÂNICA, 2004, Belém – PA. 10-13 agosto 2004, 10 p.
- Stangroom, P. CFD Modeling of Wind Flow Over Terrain. The University of Nottingham, 2004. 298p.
- Wilcox, D. C. Turbulence Modeling for CFD. DCW Industries, 2004.
- Xiao, Y.; Chao, L. CFD Approach to the Micrositing of Wind Turbines in Complex Terrain. The Research Center of Urban & Civil Engineering Disaster Prevention & Reduction, Harbin Institute of Technology Shenzhen Graduate School, Shenzhen, Guangdong, China, 2010.
- CFX Version 11.0, Solver modeling, Solver theory. ANSYS Inc., 2006.
- Loredo-Souza. A. M.; Schettini. E. B. C.; Paluch. Simulação da Camada Limite Atmosférica em Túnel de Vento. In: Möller, S. V.; Silvestrini, J. H. Turbulência. Volume 4: Rio de Janeiro. ABCM, 2004.

## 9. RESPONSIBILITY NOTICE

The following text, properly adapted to the number of authors, must be included in the last section of the paper:

The authors are the only responsible for the printed material included in this paper.